In vitro modeling of respiratory syncytial virus infection of pediatric bronchial epithelium, the primary target of infection in vivo

Rémi Villenave[a], Surendran Thavagnanam[a,b], Severine Sarlang[a], Jeremy Parker[a], Isobel Douglas[b], Grzegorz Skibinski[a], Liam G. Heaney[a], James P. McKaigue[b], Peter V. Coyle[c], Michael D. Shields[a,b], and Ultan F. Power[a,1]

[a]Centre for Infection and Immunity, School of Medicine, Dentistry and Biomedical Sciences, Queens University Belfast, Belfast BT9 7BL, Northern Ireland; [b]The Royal Belfast Hospital for Sick Children, Belfast BT12 6BE, Northern Ireland; and [c]The Regional Virus Laboratory, Belfast Trust, Belfast BT12 6BA, Northern Ireland

Edited by James Crowe, Vanderbilt University, Nashville, TN and accepted by the Editorial Board February 23, 2012 (received for review June 28, 2011)

Respiratory syncytial virus (RSV) is the major viral cause of severe pulmonary disease in young infants worldwide. However, the mechanisms by which RSV causes disease in humans remain poorly understood. To help bridge this gap, we developed an ex vivo/in vitro model of RSV infection based on well-differentiated primary pediatric bronchial epithelial cells (WD-PBECs), the primary targets of RSV infection in vivo. Our RSV/WD-PBEC model demonstrated remarkable similarities to hallmarks of RSV infection in infant lungs. These hallmarks included restriction of infection to noncontiguous or small clumps of apical ciliated and occasional nonciliated epithelial cells, apoptosis and sloughing of apical epithelial cells, occasional syncytium formation, goblet cell hyperplasia/metaplasia, and mucus hypersecretion. RSV was shed exclusively from the apical surface at titers consistent with those in airway aspirates from hospitalized infants. Furthermore, secretion of proinflammatory chemokines such as CXCL10, CCL5, IL-6, and CXCL8 reflected those chemokines present in airway aspirates. Interestingly, a recent RSV clinical isolate induced more cytopathogenesis than the prototypic A2 strain. Our findings indicate that this RSV/WD-PBEC model provides an authentic surrogate for RSV infection of airway epithelium in vivo. As such, this model may provide insights into RSV pathogenesis in humans that ultimately lead to successful RSV vaccines or therapeutics.

primary airway epithelial cells | virus–host interaction | lung epithelium model

Respiratory syncytial virus (RSV) infection is responsible for annual epidemics that cause massive morbidity and considerable mortality worldwide. It is the primary cause of hospitalization of infants in the first year of life (1). It is responsible for a spectrum of diseases ranging from rhinorrhea to life-threatening bronchiolitis and pneumonia (2). Recurrent wheezing and asthma have been observed following severe RSV lower respiratory tract infection, although a causal role for RSV in their induction remains contentious (3, 4). Despite its considerable medical importance, there are no effective and safe vaccines or RSV-specific therapeutics. Synagis, an anti-RSV F protein–specific humanized mAb, which has demonstrated prophylactic efficacy against RSV, is restricted to use in children considered at high risk of severe RSV disease. However, >50% of infants hospitalized with RSV do not fall into this category. Therefore, understanding the mechanisms by which RSV causes disease in humans remains a major medical objective.

Severe RSV-induced disease in infants is commonly characterized by wheezing, hyperinflation, atelectasis, increased mucus secretion, cyanosis, tachypnea, and consolidation (2). A number of proinflammatory cytokines and chemokines, including CXCL8, CXCL10, and CCL5, correlate positively with disease severity (5, 6). Gross and microscopic pathology from fatal cases of RSV infection are characterized by edema; small airway necrosis and sloughing; small airway plugs consisting of mucus, neutrophils, and sloughed epithelial cells; peribronchiolar and perivascular cuffing; interstitial infiltration and alveolar filling; and occasional giant cells (7–11). As a consequence of bronchiolitis, excess mucus production also is characteristic of RSV disease (12, 13). Immunohistochemistry indicated that RSV infection was restricted to airway apical epithelial cells (the principal targets of infection) and sloughed epithelial cells (10, 14). Furthermore, this infection induced the destruction of ciliated epithelial cells and appeared in general to be noncontiguous, with single or small groups of epithelial cells infected throughout the airways (9, 13). Although RSV has been studied extensively (15), the mechanisms by which it causes disease in humans remain poorly understood.

The great majority of studies on RSV pathogenesis were undertaken in animal models or continuous cell lines. Although these studies provided a number of seminal insights into RSV–host interactions, animal models, with the exception of chimpanzees, are semipermissive for RSV infection and do not reflect the range of pathologies described in RSV-infected humans. Continuous cell lines, such as HEp-2 and A549 cells, also have been used extensively to study RSV–host interactions. However, they are poorly representative of the complexities of cell interactions in the human lung. Therefore the need, for models of RSV infection that facilitate the elucidation of RSV–host interactions is compelling. In this regard, the recent advent of technology to culture primary human airway epithelial cells into physiologically authentic pseudostratified airway epithelial (HAE) cultures is very attractive (16). Indeed, such cultures already have been used to study a number of respiratory virus–host interactions, including RSV (17–23).

In the current study, we adopted this technology to develop an HAE model of RSV infection based on primary pediatric bronchial epithelial cells (21) cultured on collagen-coated, 12-mm filters in transwells at an air–liquid interface (ALI). The cells were derived from bronchial brushings of children undergoing elective surgery, and the resultant cultures were designated "well-differentiated pediatric bronchial epithelial cells" (WD-PBECs). Our data suggested that the RSV/WD-PBEC model was remarkably similar to histopathologic observations and chemokine responses in fatal and severe cases of RSV, respectively, in terms of location of infection, cytopathology, virus growth kinetics, cell sloughing, enhanced mucus production, and chemokine secretions. We also compared the consequences of WD-PBEC infection with either

Author contributions: R.V., L.G.H., M.D.S., and U.F.P. designed research; R.V. performed research; S.T., S.S., J.P., I.D., G.S., J.P.M., and P.V.C. contributed new reagents/analytic tools; R.V., L.G.H., M.D.S., and U.F.P. analyzed data; and R.V., M.D.S., and U.F.P. wrote the paper.

The authors declare no conflict of interest.

This article is a PNAS Direct Submission. J.C. is a guest editor invited by the Editorial Board.

[1]To whom correspondence should be addressed. E-mail: u.power@qub.ac.uk.

This article contains supporting information online at www.pnas.org/lookup/suppl/doi:10.1073/pnas.1110203109/-/DCSupplemental.

the prototypic strain RSV A2 or a recent clinical isolate, RSV BT2a. Although the consequences of infection were qualitatively similar for the two strains, the intensity of the responses often was higher following RSV BT2a infection. Our data suggest that the RSV strain used to study RSV pathogenesis in human tissues is important. We conclude that our model provides an authentic surrogate with which to elucidate mechanisms of RSV pathogenesis in pediatric airways.

Results

Both RSV A2 and BT2a productively infected WD-PBEC cultures and had similar growth kinetics (Fig. 1*A*). Virus titers peaked at ~5 $\log_{10}$ median tissue-culture infective dose ($TCID_{50}$)/mL at 96 h postinfection (hpi) and decreased slightly thereafter. However, on average, 4.5 times more cells (range 1.53–9.63) were infected with RSV BT2a than with RSV A2 at 144 hpi (Fig. 1*B* and Table S1). No infectious viruses were detected in the basolateral medium, indicating that virus progeny release was polarized to the apical surface. Daily monitoring of infected WD-PBECs revealed no evidence of gross cytopathic effects (CPE) or culture deterioration over 6 dpi (Fig. 2*A*). Both RSV A2 and BT2a were restricted to the apical layer of WD-PBECs (Fig. 2*B*). Compared with uninfected controls, there was no obvious deterioration in the cultures following RSV infection in terms of the number of cell layers. Moreover, ZO-1 staining suggested that tight junctions remained intact at 144 hpi (Fig. 2*C*). Both viruses primarily infected ciliated and, occasionally, nonciliated epithelial cells (Fig. 2*D* and Movie S1). Furthermore, RSV most commonly infected noncontiguous cells; not all ciliated cells were infected. However, clumps of infected cells were observed also. In contrast, goblet cells were not infected by RSV (Fig. 2*E* and Movie S2).

Although gross CPE was not evident, readily identifiable cytopathogenesis was. Syncytia, hallmarks of RSV CPE in cell line monolayers in vitro and occasionally reported in autopsy lung tissue from fatal RSV cases (7, 13), were detected invariably after infection with both RSV strains (Fig. 3 *A*–*C* and Movie S3), albeit at low frequencies (~1.18 and 2.38 per 1,000 infected cells for RSV BT2a and A2, respectively, at 144 hpi). Lumen epithelial cell sloughing is common in lung necropsy of fatal RSV cases (7–9, 11, 13), and apical washes of RSV-infected WD-PBECs contained considerably more nuclei than mock-infected controls, indicating sloughing (Fig. 3*D*). RSV BT2a induced more cell sloughing than RSV A2 (Fig. 3*E*). Many detached cells were TUNEL-positive, indicating apoptosis (Fig. 3*F*). More TUNEL-positive cells were evident in cytospins of BT2a- than A2-infected cultures; very few cells in the uninfected controls were TUNEL-positive.

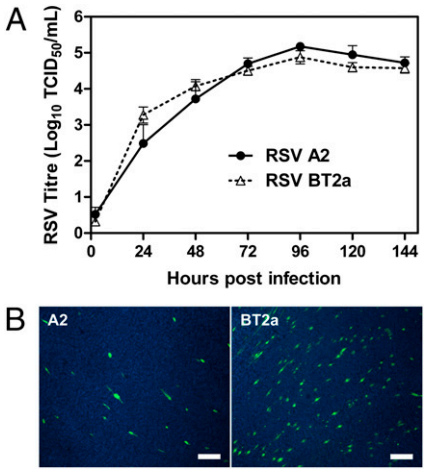

Fig. 1. Infectivity of RSV A2 and BT2a in WD-PBECs. WD-PBEC cultures ($n = 5$ donors) were infected with RSV A2 or BT2a (MOI ~4). (*A*) Virus growth kinetics determined by titrating RSV in apical washes at 24-h intervals following infection. Data are presented as mean + SEM $\log_{10}$ $TCID_{50}$/mL. (*B*) At 144 hpi, these cultures were fixed with 4% paraformaldehyde (PFA) (vol/vol) and stained with Alexa Fluor 488-conjugated anti-RSV F protein mAb (green); nuclei were counterstained with DAPI (blue). Representative *en face* micrographs of RSV A2- or BT2a-infected cultures are presented. (Magnification: 10×.) (Scale bars: 200 μm.)

Ciliated cells from the airway epithelium are found in luminal cell debris during RSV disease, consistent with their role as primary targets for RSV infection (9). To determine whether our model also displayed a loss of ciliated cells following RSV infection, cultures were trypsinized at 144 hpi, collected by cytospinning, and stained for β-tubulin (ciliated cells) (Fig. 4*A*). The percentage of ciliated cells in whole cultures was reduced by three times in the RSV BT2a- and A2-infected cultures compared with controls (Fig. 4*B*). To determine directly if ciliated cells were released from the apical surfaces of WD-PBECs following infection, cytospins of apical washes were stained with DAPI and anti–β-tubulin. At 144 hpi, more ciliated cells were present in apical rinses from the BT2a- than from the A2-infected cultures, and few were evident from uninfected controls (Fig. 4*C*). These data confirmed that RSV infection of WD-PBECs caused a loss of ciliated cells, as described in fatal cases of RSV (9).

Enhanced mucus production is a hallmark of RSV bronchiolitis (9). We therefore investigated the modulation of goblet cell content following infection. Anti-Muc5Ac staining of apical wash cytospins from infected or control WD-PBECs (144 hpi) demonstrated a large increase in mucus secretion following infection (Fig. 5*A*). Furthermore, increased goblet cell numbers were evident at 144 hpi in RSV-infected as compared with control cultures, suggesting goblet cell hyperplasia/metaplasia (Fig. 5 *B* and *C*). Interestingly, RSV BT2a induced more goblet cell hyperplasia/metaplasia than RSV A2. These data are consistent with clinical hallmarks of RSV infection.

To study components of the innate immune response to RSV in our transwell-cultured WD-PBECs, we analyzed the release of CCL5, CXCL8, CXCL10, IL-6, and TNF-related apoptosis-inducing ligand (TRAIL) to the basolateral medium (24, 96, 120, and 144 hpi) and apically (24 and 120 hpi) ($n = 5$) (Fig. 6 and Fig. S1). We also analyzed type I IFNs to determine if our RSV/WD-PBEC model reflected the very poor type I IFN responses evident following RSV infection of infants (Fig. S2) (24, 25). Because the basolateral medium was changed and apical surfaces were rinsed daily, concentrations measured corresponded to the amount of cytokines/chemokines released within the preceding 24-h period. CXCL10 (A2 and BT2a infections) and IL-6 (BT2a infection) were the only chemokines significantly up-regulated in the basolateral medium at 24 hpi compared with controls. By 96 hpi, basolateral secretions of CXCL10, TRAIL, CCL5, IL-6, and CXCL8 were significantly higher in infected than in uninfected cultures. Expression of all chemokines except CXCL8 peaked between 24 and 96 or 120 hpi and maintained high levels through the 144 hpi time point. CXCL10 was the most strongly up-regulated of the chemokines tested, particularly in RSV BT2a-infected cultures. This trend continued through 144 hpi. Similarly, TRAIL at 96 hpi and CCL5 at both 96 and 120 hpi were significantly higher in the RSV BT2a-infected cultures. Indeed, where significant differences in analyte concentrations were evident between these viruses, concentrations always were higher in RSV BT2a infections. IL-6 and CXCL8 secretion levels were similar for both viruses at all times. CXCL8 was produced at high levels following RSV infection, peaking at 120 hpi, although uninfected controls also produced large amounts. With the exception of CXCL8, similar trends in chemokine secretions were evident in apical rinses, albeit with higher baseline levels evident in mock-infected controls (Fig. S1). In contrast to the basolateral medium, there was no increase in CXCL8 concentrations in the apical washes at 120 hpi. Although direct comparisons are

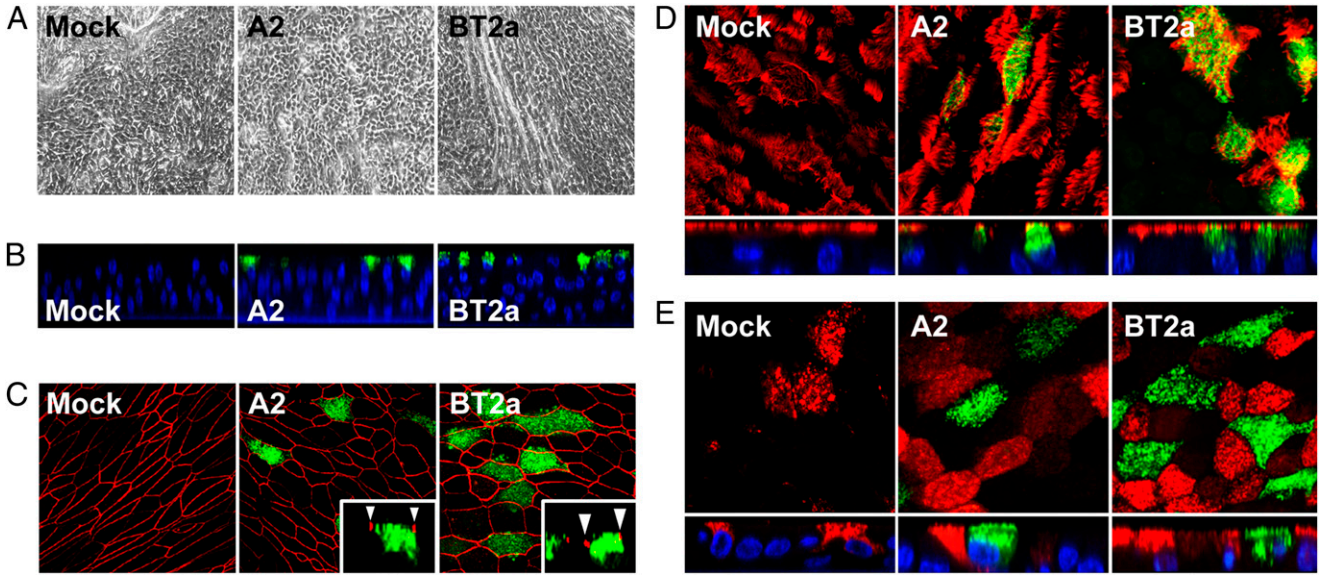

Fig. 2. RSV infection does not cause gross CPE but is restricted to apical ciliated and occasional nonciliated cells. WD-PBECs were infected as indicated in Fig. 1. (*A*) At 144 hpi, RSV- and mock-infected cultures were observed by phase-contrast microscopy for evidence of CPE. The white-cloud appearance is caused by mucus secretion. (Magnification: 10×.) (*B*) Confocal orthogonal sections of WD-PBECs, fixed at 144 hpi and stained for RSV F protein (green); nuclei were counterstained with DAPI (blue). (Magnification: 40×.) (*C*) *En face* and orthogonal (*Insets*) confocal images of RSV-infected WD-PBECs at 144 hpi, fixed and stained for RSV F protein (green) and ZO-1 (red). White arrowheads show tight junctions. (Magnification: 63×.) At 144 hpi, WD-PBECs were fixed, permeabilized, and stained for (*D*) RSV F protein (green) and β-tubulin (red) or (*E*) RSV F (green) and Muc5Ac (red). (Magnification: 63×.). Lower panels show orthogonal sections. Images are representative of five different donors.

difficult because of different harvesting protocols, absolute mean concentrations were higher in basolateral medium for CXCL10 and CXCL8; IL-6 and TRAIL concentrations were higher in apical washes; and CCL5 levels were similar in basolateral medium and apical washes. Finally, type I IFNs were not detected in basolateral medium tested at 24 or 96 hpi (Fig. S2).

Discussion

In the current study, we show that RSV infection of WD-PBECs demonstrates several characteristics that are remarkably similar to histological changes in lung tissues of fatal cases—the only RSV cases for which tissues are available—and to the pathophysiology of RSV-induced bronchiolitis. The restriction of RSV infection to apical-layer ciliated and occasional nonciliated cells is consistent with studies in adult-derived HAE cultures and histology of RSV-infected pediatric lungs (19, 26, 27). Infection of noncontiguous cells and occasional cell clumps corresponds with previous reports on lung tissues from fatal RSV and an ex vivo model of RSV infection based on human fetal tracheal ring cultures (10, 14, 28). The considerable cell sloughing from RSV-infected WD-PBECs is consistent with the fibrin-mucocellular airway occlusions that are hallmarks of RSV histopathology in infants (9). Interestingly,

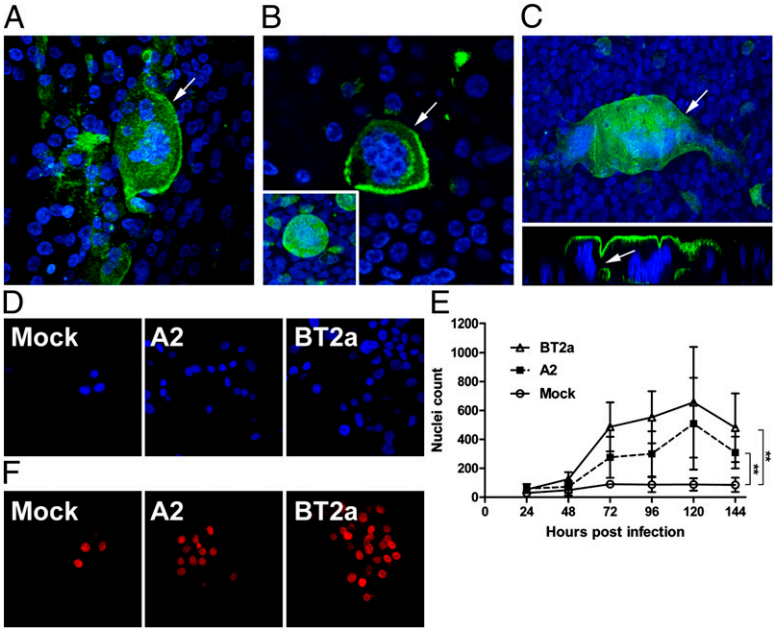

Fig. 3. RSV causes syncytia formation, apical cell sloughing, and apoptosis. WD-PBEC cultures were infected as indicated in Fig. 1. (*A*) At 144 hpi, cultures were fixed and stained with DAPI and anti-RSV F mAb to visualize nuclei (blue) and RSV-infected cells (green), respectively. Confocal data from RSV A2-infected (*A*) and BT2a-infected (*B*) cultures revealed syncytia formation after RSV infection (white arrows). Two different planes (main panel and *Inset*) are presented for BT2a infection. (Magnification: 63×.) (*C*) Large syncytium following BT2a infection. The orthogonal section (*Lower*) shows the fusion (white arrow) between two adjacent syncytia. (Magnification: 63×.) Images are representative of five different donors. (*D*) Cytospins of apical washes were performed 72 hpi, and slides were stained for DAPI to visualize apical cell sloughing. RSV infection induced considerable sloughing of cells compared with noninfected control slides, with BT2a > A2 >> uninfected cultures. (Magnification: 63×.) (*E*) Quantification of nuclei following cytospins of apical washes of RSV A2-, BT2a-, and mock-infected cultures (n = 3 donors). Values are means ± SEM. Areas under the curve were calculated for each donor and compared. $^{**}P < 0.01$. (*F*) Cytospins were performed at 72 hpi and stained for evidence of apoptosis using the TUNEL assay. BT2a-infected > A2-infected >> uninfected cultures in terms of apoptosis induction. (Magnification: 63×.)

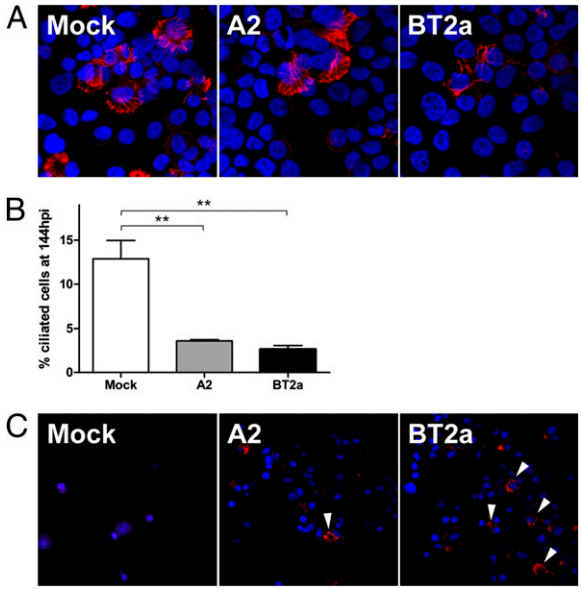

Fig. 4. RSV causes the destruction of ciliated cells. WD-PBEC cultures were infected as indicated in Fig. 1. (*A*) Cultures were trypsinized 144 hpi, and cytospins were performed. Slides were stained for β-tubulin to visualize ciliated cells left in the culture after infection. (*B*) Percentages of ciliated cells remaining in WD-PBEC cultures following RSV or mock infection (n = 3 donors) were determined by counting β-tubulin–positive cells among a total of 1,500 cells. Values are means + SEM. $^{**}P < 0.01$. (*C*) Cytospins were performed 144 hpi with apical washes and stained for β-tubulin to visualize detached ciliated cells (arrowheads).

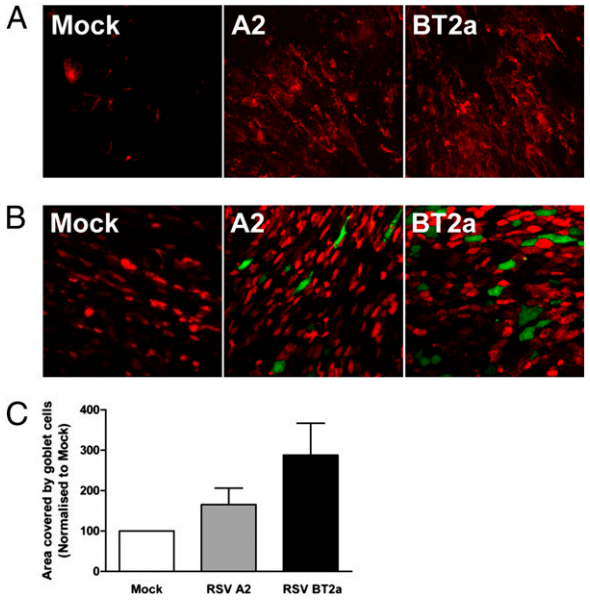

Fig. 5. RSV induces enhanced mucus secretion and goblet cell hyperplasia/metaplasia in WD-PBECs. WD-PBEC cultures were infected as indicated in Fig. 1. (*A*) Cytospins of apical washes 144 hpi. Slides were stained for MUC5AC to visualize mucus secretion following A2, BT2a, and mock infection. BT2a-infected > A2-infected >> uninfected cultures in terms of mucus secretion. (Magnification: 10×.) (*B*) Cultures were fixed with 4% PFA (vol/vol) and stained for MUC5AC (red) and RSV F protein (green) 144 hpi. Higher numbers of goblet cells were evident in BT2a- than in A2-infected cultures, and both infected cultures had demonstrably higher goblet cell content than uninfected cultures. (Magnification: 60×.) (*C*) Quantification of goblet cell hyperplasia for each condition. Values are means + SEM and represent the area covered by goblet cells in five different fields of each condition from three donors. Each condition was normalized to the mock-infected value.

apoptosis evident within the sloughed cells reflects recent observations in histology slides of RSV-infected infant lung (10). The reduction of ciliated epithelial cells within infected WD-PBEC cultures and the concomitant increase in ciliated cells among sloughed cells are consistent with characteristics of RSV bronchiolitis (9). Syncytia observed in our RSV/WD-PBEC model were remarkably similar to syncytia described recently in conducting airway tissues in RSV-infected infant lungs (7). The detection of goblet cell hyperplasia/metaplasia following RSV infection is consistent with excessive mucus production in RSV bronchiolitis (2, 12). Finally, secretions of a panel of chemokines from RSV-infected WD-PBECs are similar to levels observed in RSV-infected infants (5, 6, 10).

The infection of noncontiguous or clumps of cells with RSV and the overall extent of infection in our WD-PBEC model is consistent with previous reports with adult WD-HAE cultures, including those derived from primary adenoid and nasal epithelial cells (27). As we do, Zhang et al. (19) described restriction of infection in their WD-HAE cultures to apical ciliated cells but also more extensive infection and higher replication with recombinant RSV A2-expressing GFP [rgRSV(224)] than we observed. The epithelial cell origins (adult with/without cystic fibrosis vs. infant), specific culture conditions, and/or the virus strains used might explain these differences. Indeed, the rgRSV(224) genome contains several introduced mutations compared with wild-type RSV A2 (29).

The lack of gross WD-PBEC CPE following infection with either RSV strain is consistent with previous reports (19, 26) and suggests that culture regeneration compensates for the loss of cells through sloughing. Lung histology data from RSV-infected infants revealed areas of epithelium that were RSV positive and either relatively intact or destroyed (7, 10). Our data suggest that RSV infection alone is unlikely to be the principal cause of epithelium destruction in infants. Immune cells responding to the infection may be responsible for damage to the airway epithelium in vivo. This suggestion is consistent with the concept that much of the disease associated with RSV may be immune mediated. Future research, in which specific immune cells will be included in our RSV/WD-PBEC model, will address this possibility.

We also sought to address whether the RSV strain influenced experimental outcomes. We found that the consequences of infection of WD-PBECs were qualitatively similar for both RSV strains. However, where quantitative differences were evident, they were generally in favor of the clinical isolate. This finding may be explained, at least in part, by the increased number of cells infected by RSV BT2a relative to A2. These data contrasted with our work in monolayer PBECs, in which RSV A2 caused substantially more CPE and had higher growth kinetics than RSV BT2a (30). The cumulative data from both studies suggest that the differentiation status of the PBECs and the RSV strain used are important considerations in studying RSV pathogenesis. The striking similarities between our RSV/WD-PBEC model and aspects of the histopathology of RSV in infants suggest that this model is physiologically more authentic than the monolayer PBEC/RSV model.

Intriguingly, some ciliated cells were not infected by RSV in our model, even by 7 dpi. This result suggests that the RSV receptor is not present on all ciliated cells and/or some of them are innately or become refractory to infection. Heparan sulfate, which functions as the RSV receptor in continuous cells lines (31), is absent from the apical surface of WD-HAE cultures (18) and therefore is unlikely to function as such in WD-PBECs or in vivo. Thus, the "real" RSV receptor remains to be identified before we can address the hypothesis of receptor-associated infection restriction in some ciliated cells. Alternatively, the induction of an antiviral state in neighboring cells, as suggested by high CXCL10 secretion, may explain the limited virus spread (32). Interestingly, our data suggest that type I IFNs are not responsible for inducing such an

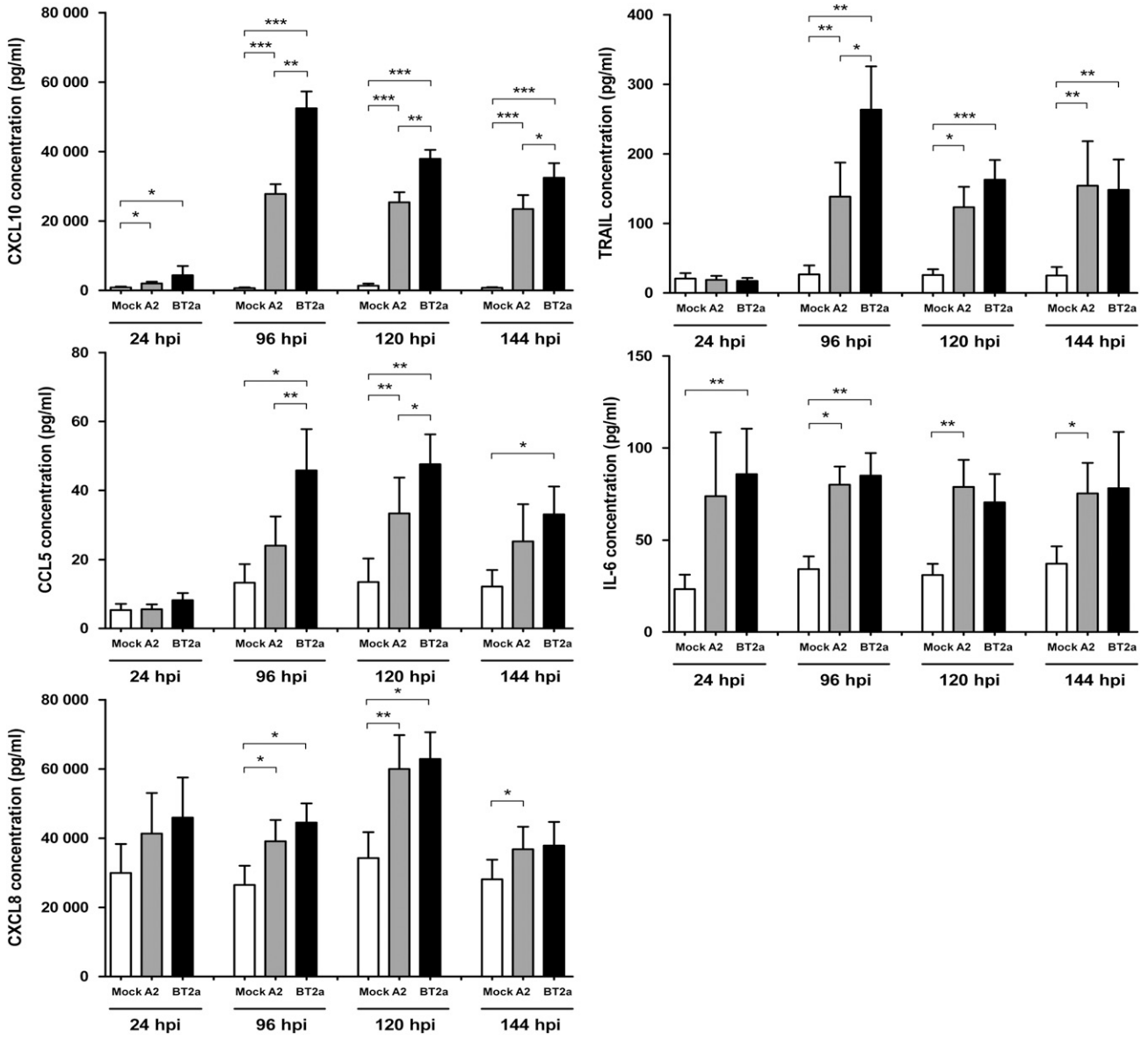

Fig. 6. Basolateral chemokine secretion induced following RSV infection. WD-PBECs were infected as indicated in Fig. 1. Chemokine secretions in the basolateral medium of RSV- and mock-infected cultures harvested at 24, 96, 120, and 144 hpi were measured (n = 5 donors). Because the medium was replaced every day, the data correspond to chemokine secretions within the preceding 24 h. Values are means + SEM. $*P < 0.05$, $**P < 0.01$, $***P < 0.001$.

antiviral state in RSV-infected WD-PBECs. Intriguingly, recent work suggests that type III IFNs may be implicated instead (33).

The detection of apoptosis among sloughed cells from RSV-infected WD-PBECs is consistent with a previous report of strong caspase 3 staining in bronchial epithelial cells from infants that died of RSV (10). As a potent inducer of apoptosis (34), the high level of TRAIL induced by infection suggests that it is implicated in RSV-induced apoptosis and corresponds with its putative role in epithelial injury during severe RSV disease (35). Further work is necessary to elucidate the role of apoptosis and TRAIL in RSV pathogenesis.

Enhanced mucus secretion, another characteristic of RSV bronchiolitis (13), was reproduced faithfully in our model. The increased numbers of goblet cells following RSV infection suggests that goblet cell hyperplasia/metaplasia might explain the increase in mucus production. Interestingly, Zhang et al. (18) also reported increased goblet cells following infection of HAE cultures with HPIV3, suggesting that this phenomenon may be common after infection with viruses from the Parmyxoviridae family. The mechanisms of RSV-induced goblet cell hyperplasia/metaplasia remain to be elucidated. However, EFG–EGF receptor interactions and exogenous IL-13 were shown recently to stimulate goblet cell hyperplasia in WD-PBEC and animal models (36–39).

Massive lung infiltration of neutrophils, monocytes, lymphocytes, and, to a much lesser extent, eosinophils is characteristic of severe RSV disease in infants (2, 7, 40, 41). Chemokines released by RSV-infected epithelial cells are undoubtedly important in this infiltration. Indeed, increased expression of IL-6, CCL5, CXCL8, and CXCL10 was evident in bronchoalveolar or nasopharyngeal lavage of infants suffering from RSV infections, compared with age-matched controls (5, 6, 10). Our data on chemokine secretion are consistent with these clinical data. Interestingly, although absolute concentrations differed, and some discrepancies were evident, the 24-h chemokine secretion trends for CCL5, CXCL8, and CXCL10 were similar to those reported by Oshansky et al. (23) at the same time point using primary normal human bronchial epithelial cells from a single donor grown at ALI.

In addition to infected cells, these authors demonstrated that exogenously added RSV F and G glycoproteins induced early chemokine responses. The much higher secretions evident from 96 hpi in the present study suggest that virus replication is the principal driver of chemokine expression, although the F and G glycoproteins produced during infection could be responsible.

In summary, our RSV/WD-PBEC model mirrors several characteristics of RSV infection in vivo. Our data also suggest that the RSV strain used to study pathogenesis may influence experimental outcomes and, thereby, our understanding of RSV pathogenesis. In conclusion, our model represents an exciting surrogate for human infection with which to elucidate mechanisms of RSV pathogenesis in epithelial cells.

Materials and Methods

Generation and Infection of WD-PBECs. PBECs were obtained from healthy children undergoing elective surgery (n = 5) (42). The generation and characterization of WD-PBEC cultures were described previously and are outlined in *SI Materials and Methods* (21, 43). Briefly, primary cells were expanded in collagen-coated flasks until almost confluent and then were transferred onto collagen-coated semipermeable (0.4-μm pore size, 12-mm diameter) membrane supports. When confluent, apical medium was removed to create an ALI. At 21 d post-ALI, when cultures formed a pseudostratified mucociliary epithelium with beating cilia and mucus production (Movie S4), they were infected in duplicate [multiplicity of infection (MOI) ∼4] with the prototypic RSV strain A2 or a recent clinical isolate, BT2a (35). The inocula or medium-only controls were added to the apical surface of the cultures and incubated for 2 h at 37 °C, 5% CO_2. Subsequently, the inoculum was removed, and the apical surface was rinsed six times with 500 μL PBS. After the final rinse, and every 24 h thereafter, the apical surface was rinsed with 500 μL PBS for 10 min at 37 °C, and the rinse was harvested, snap frozen, and stored in liquid nitrogen. In parallel, basal medium (500 μL) was harvested and stored at −80 °C until used. The harvested medium was replaced with 500 μL fresh culture medium. Apical rinses and basal medium were used to determine virus growth kinetics and cytokine/chemokine responses. All cultures were monitored daily for CPE by light microscopy. Cytospins of apical washes were performed by centrifugation and fixation with ice-cold acetone. Please refer to *SI Materials and Methods* for further details, including cytospins analyses, immunofluorescence, apoptosis assays, cytokine/chemokine quantifications, statistical analyses, and ethics.

ACKNOWLEDGMENTS. We thank the children and parents who consented to participate in this study. Funding was provided by the Public Health Agency Health and Social Care Research and Development Division, Northern Ireland and the European Social Fund.

1. Glezen WP, Taber LH, Frank AL, Kasel JA (1986) Risk of primary infection and reinfection with respiratory syncytial virus. *Am J Dis Child* 140:543–546.
2. Hall CB (2001) Respiratory syncytial virus and parainfluenza virus. *N Engl J Med* 344: 1917–1928.
3. Stein RT, et al. (1999) Respiratory syncytial virus in early life and risk of wheeze and allergy by age 13 years. *Lancet* 354:541–545.
4. Sigurs N, et al. (2005) Severe respiratory syncytial virus bronchiolitis in infancy and asthma and allergy at age 13. *Am J Respir Crit Care Med* 171:137–141.
5. McNamara PS, Flanagan BF, Hart CA, Smyth RL (2005) Production of chemokines in the lungs of infants with severe respiratory syncytial virus bronchiolitis. *J Infect Dis* 191:1225–1232.
6. Sheeran P, et al. (1999) Elevated cytokine concentrations in the nasopharyngeal and tracheal secretions of children with respiratory syncytial virus disease. *Pediatr Infect Dis J* 18:115–122.
7. Johnson JE, Gonzales RA, Olson SJ, Wright PF, Graham BS (2007) The histopathology of fatal untreated human respiratory syncytial virus infection. *Mod Pathol* 20: 108–119.
8. Kurlandsky LE, French G, Webb PM, Porter DD (1988) Fatal respiratory syncytial virus pneumonitis in a previously healthy child. *Am Rev Respir Dis* 138:468–472.
9. Aherne W, Bird T, Court SD, Gardner PS, McQuillin J (1970) Pathological changes in virus infections of the lower respiratory tract in children. *J Clin Pathol* 23:7–18.
10. Welliver TP, et al. (2007) Severe human lower respiratory tract illness caused by respiratory syncytial virus and influenza virus is characterized by the absence of pulmonary cytotoxic lymphocyte responses. *J Infect Dis* 195:1126–1136.
11. Downham MA, Gardner PS, McQuillin J, Ferris JA (1975) Role of respiratory viruses in childhood mortality. *BMJ* 1:235–239.
12. Lugo RA, Nahata MC (1993) Pathogenesis and treatment of bronchiolitis. *Clin Pharm* 12:95–116.
13. Neilson KA, Yunis EJ (1990) Demonstration of respiratory syncytial virus in an autopsy series. *Pediatr Pathol* 10:491–502.
14. Wright C, Oliver KC, Fenwick FI, Smith NM, Toms GL (1997) A monoclonal antibody pool for routine immunohistochemical detection of human respiratory syncytial virus antigens in formalin-fixed, paraffin-embedded tissue. *J Pathol* 182:238–244.
15. Chanock R, Roizman B, Myers R (1957) Recovery from infants with respiratory illness of a virus related to chimpanzee coryza agent (CCA). I. Isolation, properties and characterization. *Am J Hyg* 66:281–290.
16. Gray TE, Guzman K, Davis CW, Abdullah LH, Nettesheim P (1996) Mucociliary differentiation of serially passaged normal human tracheobronchial epithelial cells. *Am J Respir Cell Mol Biol* 14:104–112.
17. Matrosovich MN, Matrosovich TY, Gray T, Roberts NA, Klenk HD (2004) Human and avian influenza viruses target different cell types in cultures of human airway epithelium. *Proc Natl Acad Sci USA* 101:4620–4624.
18. Zhang L, et al. (2005) Infection of ciliated cells by human parainfluenza virus type 3 in an in vitro model of human airway epithelium. *J Virol* 79:1113–1124.
19. Zhang L, Peeples ME, Boucher RC, Collins PL, Pickles RJ (2002) Respiratory syncytial virus infection of human airway epithelial cells is polarized, specific to ciliated cells, and without obvious cytopathology. *J Virol* 76:5654–5666.
20. Lopez-Souza N, et al. (2009) In vitro susceptibility to rhinovirus infection is greater for bronchial than for nasal airway epithelial cells in human subjects. *J Allergy Clin Immunol* 123:1384–1390.
21. Villenave R, et al. (2010) Cytopathogenesis of Sendai virus in well-differentiated primary pediatric bronchial epithelial cells. *J Virol* 84:11718–11728.
22. Oshansky CM, Krunkosky TM, Barber J, Jones LP, Tripp RA (2009) Respiratory syncytial virus proteins modulate suppressors of cytokine signaling 1 and 3 and the type I interferon response to infection by a toll-like receptor pathway. *Viral Immunol* 22: 147–161.
23. Oshansky CM, Barber JP, Crabtree J, Tripp RA (2010) Respiratory syncytial virus F and G proteins induce interleukin 1alpha, CC, and CXC chemokine responses by normal human bronchoepithelial cells. *J Infect Dis* 201:1201–1207.
24. Hall CB, Douglas RG, Jr., Simons RL, Geiman JM (1978) Interferon production in children with respiratory syncytial, influenza, and parainfluenza virus infections. *J Pediatr* 93:28–32.
25. Melendi GA, et al. (2010) Breastfeeding is associated with the production of type I interferon in infants infected with influenza virus. *Acta Paediatr* 99:1517–1521.
26. Mellow TE, et al. (2004) The effect of respiratory synctial virus on chemokine release by differentiated airway epithelium. *Exp Lung Res* 30:43–57.
27. Wright PF, et al. (2005) Growth of respiratory syncytial virus in primary epithelial cells from the human respiratory tract. *J Virol* 79:8651–8654.
28. Henderson FW, Hu SC, Collier AM (1978) Pathogenesis of respiratory syncytial virus infection in ferret and fetal human tracheas in organ culture. *Am Rev Respir Dis* 118: 29–37.
29. Hallak LK, Spillmann D, Collins PL, Peeples ME (2000) Glycosaminoglycan sulfation requirements for respiratory syncytial virus infection. *J Virol* 74:10508–10513.
30. Villenave R, et al. (2011) Differential cytopathogenesis of respiratory syncytial virus prototypic and clinical isolates in primary pediatric bronchial epithelial cells. *Virol J* 8: 43.
31. Bourgeois C, Bour JB, Lidholt K, Gauthray C, Pothier P (1998) Heparin-like structures on respiratory syncytial virus are involved in its infectivity in vitro. *J Virol* 72: 7221–7227.
32. Luster AD, Unkeless JC, Ravetch JV (1985) Gamma-interferon transcriptionally regulates an early-response gene containing homology to platelet proteins. *Nature* 315: 672–676.
33. Okabayashi T, et al. (2011) Type-III interferon, not type-I, is the predominant interferon induced by respiratory viruses in nasal epithelial cells. *Virus Res* 160:360–366.
34. Wiley SR, et al. (1995) Identification and characterization of a new member of the TNF family that induces apoptosis. *Immunity* 3:673–682.
35. Bem RA, et al. (2009) Potential role of soluble TRAIL in epithelial injury in children with severe RSV infection. *Am J Respir Cell Mol Biol* 42:697–705.
36. Park JA, Tschumperlin DJ (2009) Chronic intermittent mechanical stress increases MUC5AC protein expression. *Am J Respir Cell Mol Biol* 41:459–466.
37. Thavagnanam S, et al. (2011) Effects of IL-13 on mucociliary differentiation of pediatric asthmatic bronchial epithelial cells. *Pediatr Res* 69:95–100.
38. Tamaoka M, et al. (2008) The epidermal growth factor receptor mediates allergic airway remodelling in the rat. *Eur Respir J* 32:1213–1223.
39. Kibe A, et al. (2003) Differential regulation by glucocorticoid of interleukin-13-induced eosinophilia, hyperresponsiveness, and goblet cell hyperplasia in mouse airways. *Am J Respir Crit Care Med* 167:50–56.
40. Jones A, et al. (2002) Neutrophil survival is prolonged in the airways of healthy infants and infants with RSV bronchiolitis. *Eur Respir J* 20:651–657.
41. Yasui K, et al. (2005) Neutrophil-mediated inflammation in respiratory syncytial viral bronchiolitis. *Pediatr Int* 47:190–195.
42. Doherty GM, et al. (2003) Non-bronchoscopic sampling and culture of bronchial epithelial cells in children. *Clin Exp Allergy* 33:1221–1225.
43. Parker J, et al. (2010) A 3-D well-differentiated model of pediatric bronchial epithelium demonstrates unstimulated morphological differences between asthmatic and nonasthmatic cells. *Pediatr Res* 67:17–22.